A STUDY OF FATIGUE NOTCH SENSITIVITY OF 2014-T AND 7075-T AT ELEVATED TEMPERATURES

Thesis by

George Stalk

Captain, United States Air Force

In Partial Fulfillment of the Requirements

For the Degree of

Aeronautical Engineer

California Institute of Technology

Pasadena, California

1955

ACKNOWLEDGEMENTS

The author is deeply grateful to Dr. E. E. Sechler, who suggested this research topic, and whose guidance and constructive criticism throughout the course of the investigation have been a constant source of inspiration.

The author also wishes to acknowledge the helpful suggestions and efforts in the preparation of this report as follows: Dr. M. L. Williams and Dr. H. Lurie for their discussions concerning the research program, and Mr. Milton Wood for the test equipment and untold assistance; Mr. Marvin Jessey for his aid in the electronic design; Mr. C. A. Bartsch and the GALCIT Machine Shop personnel for the preparation of the specimens and repairs of the equipment, and Mrs. Betty Wood for presentation of data and drawings of the equipment.

The author is further indebted to Captain G. T. James, Jr., USAF, his associate in this study.

SUMMARY

This experiment was conducted to investigate the reversed.-bending fatigue notch sensitivity of 2014-T and 7075-T at elevated temperatures.

Tests were conducted. on three configurations of specimens which had external circumferential notches, and on one configuration of un-notched specimens.

It was determined that the experimental stress concentration factor for both alloys, at room and. elevated temperatures, increases vith decreasing notch radius.

At room and elevated temperatures, the fatigue notch sensitivity for both 2014-T and 7075-T, generally increases with increasing notch radius.

The fatigue notch sensitivity factor and the experimental stress concentration factor for 2014-T increases with temperature, reaches a maximum in the range of 250°F to 350°F and then decreases at 400°F.

The experimental stress concentration factor for 7075-T increases almost linearly from room temperature to 400°F.

The fatigue notch sensitivity factor for 7075-T increases almost linearly from room temperature to 400°F, but only the 0.09 inch radius notch configuration shows a tendency to level off.

TABLE OF CONTENTS

LIST OF FIGURES

LIST OF TABLES

I. INTRODUCTION

Although no analytic solution to the fatigue life of a particular material exists, there is a possibility, through experimental testing, to determine qualitatively the effect of size, shape, surface finish, and surface coating of a material on its fatigue life.

This experiment was conducted to investigate the variation of notch sensitivity of certain light alloys at elevated temperatures as compared to their notch sensitivity at room temperature.

Notch sensitivity is defined as a measure of the degree of agreement between the experimental stress concentration factor and the theoretical stress concentration factor for a particular specimen of given size and material containing a stress concentrator of given size and shape. (Ref. 1, p.5)

Thus: $$q = \frac{K_f - 1}{K_t - 1}$$

Where: q = notch sensitivity

K_f = experimental stress concentration factor

K_t = theoretical stress concentration factor

Because they have desirous physical characteristics and are being used widely as structural members in high speed aircraft, 2014-T and 7075-T were chosen for the experiment.

Four configurations of specimens were tested, using an R. R. Moore rotating bending machine. One configuration was un-notched and the other three had circumferential notches with notch radii of 0.01 inch, 0.02 inch, and 0.09 inch respectively. The minimum root diameters of all the specimens were 0.300 inch, and the specimens conformed to the ASTM standard. (See Fig. 7 and Ref. 1, p 30) Testing was performed at room temperature, 200°F and 400°F.

The investigation was conducted by the author in the Guggenheim Aeronautical Laboratory, California Institute of Technology, Pasadena, California, under the supervision of Dr. E. E. Sechler during the period June, 1954 to May, 1955.

II. DESCRIPTION OF APPARATUS AND SPECIMENS

The test apparatus consisted of several distinct component systems, and for clarity, these systems will be described individually in the remainder of this section.

1. Fatigue Testing Machine.

Pure-bending, rotating beam type fatigue machines were used for conducting the test. The eight machines that were used in this experiment were R. R. Moore machines which were manufactured by the Baldwin-Southwark Co. Four of the machines were on hand during the initial phase of this experiment, and four new machines were delivered in December, 1954 and integrated into the test program in January, 1955. The new machines were modified slightly to compare with the old machines. The modification was simply a disconnect and switch wired into the field of the electric motor. This offered a speed control feature when a variable resistor was wired through the disconnect; however, the speed control feature was not used in this test. The actual speeds of operation varied from one machine to another, the slowest running at 8,000 rpm and the fastest at 14,000 rpm. In this range, speed has a negligible effect on fatigue life; consequently, no attempt was made to synchronize the machines. (See Fig. 1 for photograph of a R. R. Moore machine.)

The nominal stress obtained per pound of load applied is calculated as follows:

$$S = \frac{16\ WL}{\pi\ d^3}$$

The specimens tested had a minimum diameter of 0.300 inches and L, a fixed dimension of the machine, was 4 inches. This gives:

$S = 755\ W$ psi, where W is the applied load in pounds.

Appendix I is offered as an aid to those who may use the machines and equipment in the future. Operational problems encountered and solutions to these problems are presented.

2. Furnaces.

The first furnace was designed and constructed by the author and Capt. James, whose work in a related field required the use of the same equipment. Eight additional furnaces were built by the GALCIT Machine Shop personnel.

A minimum spacing of 1.7 inches between the bearing housings caused some difficulty in the design of the furnaces. The vertical walls had to be rather thin to allow adequate heat coverage on the specimen; consequently, the heat losses were high and a high heat input was required. In addition, the bearings would attain a high temperature and bearing seizure might be encountered. Capt. James had no bearing trouble, but the author experienced some difficulty while running tests with loads less than 11 pounds. The bearing housings were approximately horizontal at these loads and the oil was forced out the oil overflow holes at the rear of the housings due to the extreme heat of the barrels. Thus, the front bearings did not receive adequate lubrication and bearing seizure resulted during a few test runs.

The furnace was constructed from 5-inch transite pipe, and layers of 1/8 inch asbestos sheeting were laminated to give an inside diameter of approximately 3 inches. The ends of the furnace were enclosed by one layer of asbestos and a sheet of 0.020-2024-T. (See Fig. 2 for details of the furnace. Figs. 3 and 4 are photographs of the furnace mounted in the open and closed position.)

After considerable experimenting with various types of element windings, a flat wound coil of 23-gage Tophet C wire was found to give a satisfactory spanwise temperature distribution across the specimen. The elements consisted of two 48 inch sections of wire, one mounted in the top half with four supports, and one mounted in the bottom half with one retainer, and connected together as a series circuit. Results of calibrations are given in Part II.

Although the furnaces were designed to attain 700°F, it is believed that furnace deterioration would be rather rapid at this temperature. At 400°F, the average coil life was in the thousands of hours and the furnaces remained in satisfactory condition.

Forced air from the electric motors was prevented from blowing past the furnaces by deflectors. These deflectors were fashioned from sheet metal or pasteboard.

Six R. R. Moore machines were mounted with furnaces leaving two machines for room temperature testing.

3. Furnace Thermocouple.

The thermocouple wires were inserted into the oven through a two-hole ceramic insulator. The insulator was fastened securely in a threaded brass tube by a set screw, and the brass tube was supported by a bracket on top of the furnace. (See Fig. 2) Positioning of the thermocouple was accomplished by inserting a calibration specimen into the oven with the thermocouple just touching the specimen. Then the set screw was tightened and the thermocouple was withdrawn from the specimen by a certain number of turns on a knurled nut. Pressure against the nut was maintained by a compression spring.

The first thermocouples used were of iron and constantin, but the high air temperature inside the furnace caused a low life expectancy. Chromel and Alumel (22-gage) were used during the latter testing period and resulted in satisfactory operation.

The thermocouple sensing juncture was formed by welding.

The thermocouple leads to the temperature control units were insulated duplex (20-gage) Chromel-Alumel. The thermocouple and lead wires were joined approximately 2 inches above the ceramic insulator. (See Fig. 4)

4. Temperature Control Units.

The furnace temperature was controlled by a pyrometer into which the thermocouple voltage was impressed. The pyrometer actuated a double pole single throw relay which was located in the furnace circuit.

The range of the pyrometers used was much less than the range of air temperatures to be encountered in the furnaces. Consequently, a shunt resistance was connected across the thermocouple terminals to increase the range of control. The shunt resistances were chosen such that the pyrometer settings would approximate the desired specimen temperature.

Two of the pyrometers used were Sym-Ply-Trol's, manufactured by Assembly Products, Inc., Chagrin Falls, Ohio, and the other four were the Series J. Gardsman, made by West Instrument Corporation, 525 North Noble Street, Chicago 22, Illinois.

5. Circuitry.

A ballast resistor was placed across a relay in the furnace line to allow a decreased current when the relay was opened. This relay was actuated by the pyrometer. This arrangement offered a decreased amplitude of temperature variation in the furnace which would otherwise be approximately 15°F at the 400°F level. In addition to this, the life of the element coils was increased considerably.

A second relay was incorporated in the furnace circuit to provide complete removal of voltage from the heater elements when the specimen failed. This relay was actuated by the cut-off switch on the R. R. Moore machine.

A powerstat was used in the furnace circuit to provide minimum adequate current to the heater elements. This lengthened the life of the coils and also contributed to a small temperature spread by decreasing the overshoot.

Fig. 6 shows in detail the complete circuitry of one R. R. Moore machine and one furnace.

Power was brought to a table on which were located the powerstats, relays, pyrometers, ballast resistors, and circuit breakers. The wiring of the machines to the table was provided with plugs for a quick disconnect. This provided portability and permitted power removal from certain parts for repairs.

6. Specimens.

The 2014-T specimens were made from a forged butt of a propeller blade. The specimens were obtained from the material well in from the surface to avoid forging effects.

The 7075-T specimens were made from a 3/4 inch rolled plate. The material near the edges of the plate was not used.

All specimens were cut with the grain along the longitudinal axis.

The un-notched specimens were polished with 600 Emery paper followed by levigated alumina using a slow lathe rotation and a rapid manual longitudinal motion. The finished specimen had a 5 μ surface finish. Close visual checks of each specimen and spot checks of surface finish were made with a Physicists Research Co., Profilometer Type Q Model.

The circumferential notches on the notched specimens were first polished with 600 Emery paper. For the smaller radius notches the Emery paper was wrapped around a piece of piano wire. This was followed by polishing with a string, soaked in a mixture of kerosene and levigated alumina.

The surface finish was checked for proper smoothness by visually comparing it with that of the un-notched specimens.

III. TEST PROCEDURE

The first phase of the test program was to calibrate the furnaces. This was done in two steps. The first was to determine the spanwise temperature distribution along the specimen at each test temperature level, and the second was to determine the proper pyrometer setting for the desired specimen temperature in the actual test set-up.

In the calibration for spanwise temperature distribution, five thermocouples were positioned on a specimen which was mounted in the machine. One thermocouple was located at the center of the specimen, two were located 1/4 inch to each side of the center, and two were located 3/4 inch to each side of center. Each thermocouple was secured firmly under the head of a screw and on the surface of the specimen. The calibration was accomplished a number of times to determine whether repeatability of results could be obtained and to get averages. A Leeds and Northrup Portable Precision Potentiometer Number 8662 was used to determine the temperature of the specimen at the thermocouple positions. The following approximate percentage variations of the off center thermocouples, relative to the center thermocouple temperature, were obtained:

Temperatures, ^{o}F	1/4 inch thermocouple	3/4 inch thermocouple
200	1.7%	4.5%
400	3.0%	3.7%
600	2.9%	5.5%

The actual testing was a dynamic one, while the calibration was conducted under a static condition. A dynamic calibration would have required an installation of slip rings; however, due to the fact that the specimens were of a very small size, and the close clearances present between the furnace and bearing housing, this type of calibration was not considered feasible. It was assumed that the spanwise temperature distribution during operation would be the same as that determined by the static calibration.

Most of the un-notched specimens broke within the area of $\pm$ 1/4 inch from the center of the specimen and all of the notched specimens broke at the center. Consequently, the region within 1/4 inch of the center was of primary interest. The calibration showed that the maximum variation at the 1/4 inch thermocouple was 3%, and it would seem very unlikely that under the worst possible combination of factors that the temperature variation could exceed 5%.

All the furnaces were constructed to the same specifications and the coils were wound alike; therefore, it was assumed that the spanwise temperature distribution, determined by the calibration, would exist in each furnace.

To determine the pyrometer setting for controlled temperature in the furnace only one thermocouple was placed at the center of the specimen. Again it was mounted securely under the head of a screw and on the surface of the specimen. The portable potentiometer used in the calibration for spanwise temperature distribution was also used for this calibration. The calibration consisted of adjusting the pyrometer setting until the desired temperature was obtained and stabilized at the desired level.

The furnace thermocouple position relative to the specimen had some effect on the specimen temperature. Consequently, the thermocouple position was established by backing the thermocouple from the specimen a certain number of turns on the positioning nut and was not moved after calibration. If a thermocouple was replaced another calibration was accomplished.

The pyrometer settings had some looseness in the adjusting mechanism.

At the 200°F setting this was unimportant, but at 400°F it was found that moving the setting, then resetting the pyrometer at the calibrated setting, would give a temperature change of 5 - 10 degrees. Therefore, once the furnace was calibrated for 400°F the pyrometer was not reset without a subsequent calibration.

Because of the type of temperature control there was some oscillation of temperature about the desired level. Prior to installation of the ballast resistors, described in Part II, this oscillation was $\pm$ 2°F or a $\pm$ 1% temperature variation at 200°F. After the installation, the fluctuation was approximately $\pm$ 1°F. No distinction is made between specimens tested under the two conditions. The fluctuation at 400°F was about $\pm$ 3°F or $\pm$3/4%. All testing at 400°F was accomplished after the installation of the ballast resistors.

The pyrometer setting calibration was also a static calibration. It was assumed that the effect on the calibrated temperature during operation was negligible.

The initial program included a test level of 600°F, but after the program got under way, it was decided that this level was out of the useful range of the alloys. Therefore, the 600°F level was abandoned and the specimens allocated for this temperature were distributed among the other three levels.

The actual running of tests required the usual preliminary preparations, such as setting the revolution counter and placing the desired load on the tray. After the preliminaries, however, the procedure varied with the temperature level.

At room temperature, as at the elevated temperatures, it was required to start the machine first and then apply the load to the knife edges. At room temperature, this procedure alleviated the danger of damage to the specimen by transient vibrations during acceleration. At the elevated temperatures, starting first also prevented the possibility of excessive creep at the high stress levels. The latter reason was investigated at the 400°F level. As a matter of interest, the load was placed on the knife edges before the machine was started. During the short interval required to start the machine, the specimen was permanently deformed and had to be discarded.

The time required to attain a given level, and stabilize at this level, was determined during the calibration. Starting with the specimen and bearing housings at room temperature, the time required was 45 minutes for the 200°F level and 1.5 hours for the 400°F level. If the specimen was placed in the barrels immediately after another had broken, these times could be reduced to 30 minutes.

Any specimen that received a rest period, or underwent a visible transient vibration, was discarded.

IV. DATA REDUCTION AND DISCUSSION OF RESULTS

Table I through XXIV presents the stress vs. number of cycles at fracture for the two alloys at the various levels of temperatures. These results are plotted in Figs. 8 through 13. As was expected, the scatter was prominent; however, a curve was drawn for each configuration of specimen at each level of temperature to indicate the average S-N curve. The actual spread in the data can readily be seen in these curves, which contain all of the test data.

Some possible sources of error or deviations which would cause this scatter are as follows:

a) Vibration of rotating parts.

b) Unavoidable impacts on specimen during loading.

c) Lag between loading and cycle counter setting.

d) Variation in machining.

e) Non-homogeneity of metal.

f) Uncertainty in the measurement of load, load arm, and specimen diameter.

All of the factors, listed above, were controlled as well as possible. One of the larger factors present in causing scatter is non-homogeneity of material. (Ref. 4, p.75)

Uncertainty in the measurement of load, load arm, and specimen diameter can be calculated. (Ref. 4, p.14) As the load decreases, this percentage error increases. Using the lowest test load of 8.44 pounds, and L and D the same as given earlier, the percentage error was 0.58%. The stress resulting from this load, with its maximum possible deviation, is 6370 ± 37 psi.

Photographs of failed specimens have not been included. The fractures were typical and Reference 2, and 3 present views of these fractures for un-notched and notched specimens respectively.

Although the experimental stress concentration factor, K_f, will increase for decreased loading (Ref. 5, p.69) it was decided to use an average value of K_f for analysis of the notch sensitivity factor. K_f was determined at five positions of fatigue life for each configuration of notched specimens at each level of temperature.

The ratio K_f is defined as:

$$K_f = \frac{\text{Fatigue strength of un-notched specimens at N cycles}}{\text{Fatigue strength of notched specimens at N cycles}}$$

Simple averages of K_f were calculated and are presented in Tables XXV and XXVI and plotted in Figs. 14 and 16.

The theoretical stress concentration factor, K_t, was determined by calculating the stress concentration factor for a deep notch (Ref. 6, p.92) and determining the stress concentration factor for a shallow notch (Ref. 6, p.56) then combining the two values, using Neuber's method, to find the expression for a notch of arbitrary depth. (Ref. 6, p.7) The largest variation in K_t, using a range of Poisson's ratio from 0.3 to 0.5, is 1%; consequently, a Poisson's ratio of 0.3 was used throughout the remainder of the calculations.

The equations to determine the theoretical stress concentration factor were only variable in Poisson's ratio, radius of notch, root diameter and depth of notch. The effect of the test temperature on the geometry of the specimen was negligible and the variation due to Poisson's ratio was calculated and found to be negligible. No information was available for determining the variation of K_t at elevated temperatures; therefore, it was decided to use the values of K_t calculated at room temperatures for the levels of 200°F and 400°F. Values of K_t for each configuration of notched specimens are presented in Table XXV and XXVI.

The notch sensitivity factor, q, was determined from the equation:

$$q = \frac{K_f - 1}{K_t - 1} \quad \text{(Ref. 5, p.70)}$$

The values of q are presented in Tables XXV and XXVI and are plotted against temperature in Figs. 15 and 17.

The experimental stress concentration factor was higher for the small radius notches and, in general, the notch sensitivity factor was higher for the larger radius notches as was expected. (Ref. 5, p.69-71)

The curves of K_f vs. temperature (Fig. 14) for 2014-T shows that K_f has a maximum value at some level of temperature in the range of 250°F to 350°F. All three configurations of notched specimens indicate the same tendency.

For 7075-T, K_f increased almost linearly for each configuration of notch to 400°F. (Fig. 16) The average slopes of the curves appear to be nearly equal.

The curves of q vs. temperature for 2014-T (Fig. 15) indicate the same tendency as the curves of K_f vs. temperature for 2014-T. The crossing of the 0.01 inch radius notch and 0.02 inch radius notch curves can be attributed to experimental scatter and insufficient data. The S-N curves, from which the q's were eventually plotted, are average curves. With more data, a statistical approach could have been used in plotting the S-N curves, and this crossing might not have occurred.

For 7075-T, q increased almost linearly for the 0.01 inch radius notch and the 0.02 inch radius notch to 400°F. However, for the 0.09 inch radius notch, q increased more rapidly with the temperature than did the other two configurations, but the curve is definitely non-linear and concave.

For 2014-T, the notch sensitivity for the 0.09 inch radius notch was greater than 1.0 at 200°F; for 7075-T, q was greater than 1.0 at 200°F and 400°F for the same notch radius. By assuming that K_t is constant for all elevated temperatures, the notch sensitivity is a function of experimental stress concentration factor only. Thus, it seems plausible that if the configuration being tested has a q close to 1.0 at room temperature, and with K_f increasing with temperature, that q will eventually be greater than 1.0, unless the theoretical stress concentration factor increases also. As stated earlier, for lack of information, the theoretical stress concentration factor is assumed to remain constant for the temperature levels tested. The plots of q vs. temperature for the two alloys is only offered as a qualitative analysis.

V. CONCLUSIONS

The following conclusions may be drawn from the results obtained in this work:

1. The experimental stress concentration factor for 2014-T and 7075-T increases with decreasing notch radius at room and elevated temperatures.

2. At room and elevated temperatures, the fatigue notch sensitivity for both 2014-T and 7075-T, generally, increases with increasing notch radius.

3. The experimental stress concentration factor for 2014-T increases with temperature but has a maximum value in the range of 250°F to 350°F and then decreases with temperatures to 400°F.

4. The experimental stress concentration factor for 7075-T increases almost linearly in the range of room temperature to 400°F.

5. The notch sensitivity factor for 2014-T increases with temperature, has a maximum value within the range of 250°F to 350°F and then decreases with temperature to 400°F.

6. The notch sensitivity factor for 7075-T increases almost linearly from room temperature to 400°F, but only the 0.09 radius notch configuration shows a tendency to level off.

It is recommended that further fatigue testing be conducted for the purpose of making a statistical approach to determining the S-N curves.

It is further recommended that fatigue tests be conducted at temperature levels in the range of 250°F to 350°F, using 2014-T to determine the maximum values of K_f and q of the three configurations of external circumferential notches.

REFERENCES

1. "ASTM" Special Technical Publication, No. 91, Manual on Fatigue Testing, 1949, p. 30.

2. Cooley, James S., Lt. Comdr., USN, "Reversed Bending Fatigue Properties of 25-ST, 75-ST, and 76-ST Aluminum Alloys", California Institute of Technology, AE Thesis, 1949.

3. Dervishyan, Aram O., "Fatigue Stress Concentration Studies on Aluminum Alloys", California Institute of Technology, AE Thesis, 1952.

4. Eprenuian, E. and Mehl, R. F., "Investigation of Statistical Nature of Fatigue Properties", NACA-TN 2719, June 1952.

5. Grover, H. J., Gordon, S. A., and Jackson, L. R., "Fatigue of Metals and Structures", NAVAER 00-25-534, Bureau of Aeronautics, Department of the Navy, 1954.

6. Neuber, Heinz, "Theory of Notch Stresses", Published by Edwards Brothers, Inc., Ann Arbor, Michigan, 1946.

APPENDIX I

OPERATION OF R. R. MOORE MACHINES

Machining quality of specimens is the most important factor for satisfactory operation of the R. R. Moore machine. Test specimens for rotating-beam machines must be prepared very carefully to insure that the grip ends are accurate and the axis of one end coincides with the axis of the other end so that the specimen will run true in the machine. (Ref. 1, p.43) If either of these factors is not within the tolerance, severe vibrations will occur during the test-run. The specimen will either break at the grip end, turn the machine off without breaking; or, if fractured, give an erroneous reading for the test. Specimen machining should be carefully controlled.

If too much oil is used in the bearing housings at room temperature, the bearing action on the oil will generate enough heat to warm the specimens. For smoothest operation and proper specimen temperature, use as little oil as possible. If oil drains out the overflow, there is too much oil in the barrels. At elevated temperatures, however, the reverse procedure must be used. The barrels become very hot and require more lubrication for proper bearing functioning. Therefore, at these elevated temperatures, enough oil is used to show a drain at the oil overflow. This will be approximately one oil cup full at 200°F, and two oil cups full at 400°F every twenty-four hours of operation. However, it is very important that a visual oil drain is present.

Unless an improved bearing lubrication system is designed, operation of the machines at temperatures over 300°F with less than 11 pounds of load in the tray should be avoided. Under this condition, the housings will be almost horizontal, and the extreme heat of the barrels will force the oil out the oil overflow holes at the rear of the housings. Thus, it would be necessary to add oil continuously for proper lubrication of the front bearings.

Eight parts of regular SAE 10 motor oil and one part of "Bardahl" was used as the lubricant for the bearings.

Care of the electric motors includes adding cup grease occasionally and periodically checking the motor commutator brushes. The brushes should be replaced as determined by the wear.

The rotation counters should occasionally be lubricated with SAE 10 oil.

TABLE I

S-N Data for 2014-T

Room Temperature, Un-Notched

Specimen Number	Applied Load lb	S Stress psi	N No. of Cycles X 10^{-3}
1	50	37,700	98
2	45	33,950	251
3	40	30,200	571
4	37.5	28,300	3,132
5	"	"	647
6	"	"	476
7	"	"	1,576
8	36	27,150	975
9	35	26,400	10,581
10	"	"	3,238
11	"	"	4,198
12	34	25,650	25,002
13	30	22,650	29,521
14	28	21,100	97,605

TABLE II

S-N Data for 2014-T

Room Temperature, 0.09 Radius Notch

Specimen Number	Applied Load lb	S Stress psi	N No. of Cycles X 10^{-3}
1	40	30,200	76
2	35	26,400	246
3	30	22,650	3,974
4	"	"	385
5	25	18,850	5,180
6	"	"	8,470
7	24	18,100	4,144
8	"	"	23,886
9	"	"	14,663
10	23.5	17,720	61,305
11	22.5	17,000	74,471
12	20	15,100	74,850*

* Removed before failure.

TABLE III

S-N Data for 2014-T

Room Temperature, 0.02 Radius Notch

Specimen Number	Applied Load lb	S Stress psi	N No. of Cycles X 10^{-3}
1	35	26,400	44
2	30	22,650	133
3	25	18,850	271
4	22.5	17,000	719
5	21	15,850	469
6	20	15,100	12,060
7	18	13,580	31,905

TABLE IV

S-N Data for 2014-T

Room Temperature, 0.01 Radius Notch

Specimen Number	Applied Load lb	S Stress psi	N No. of Cycles X 10^{-3}
1	25	18,850	137
2	20	15,100	373
3	17.5	13,200	990
4	15	11,320	6,843
5	14.5	10,920	611
6	14	10,560	27,318
7	10	7,550	95,650

TABLE V

S-N Data for 2014-T

200°F, Un-Notched

Specimen Number	Applied Load lb	S Stress psi	N No. of Cycles X 10^{-3}
1	45	33,950	288
2	40	30,200	1,133
3	"	"	293
4	35	26,400	683
5	"	"	1,195
6	34	25,650	880
7	33.5	25,250	674
8	33	24,900	2,141
9	32.5	24,500	4,009
10	32	24,150	2,162
11	31.5	23,750	995
12	30	22,650	5,261
13	25	18,850	24,356

TABLE VI

S-N Data for 2014-T

200°F, 0.09 Radius Notch

Specimen Number	Applied Load lb	S Stress psi	N No. of Cycles X 10^{-3}
1	35	26,400	127
2	30	22,650	455
3	27.5	20,750	472
4	25	18,850	1,211
5	22.5	17,000	3,674
6	20	15,100	6,794
7	"	"	18,359
8	19	14,320	19,220
9	18	13,580	22,432

TABLE VII

S-N Data for 2014-T

200°F, 0.02 Radius Notch

Specimen Number	Applied Load lb	S Stress psi	N No. of Cycles X 10^{-3}
1	25	18,850	154
2	22.5	17,000	252
3	20	15,100	907
4	17.5	13,200	3,286
5	15	11,320	6,245
6	"	"	8,028
7	14	10,560	33,345
8	13	9,820	20,100

TABLE VIII

S-N Data for 2014-T

200°F, 0.01 Radius Notch

Specimen Number	Applied Load lb	S Stress psi	N No. of Cycles X 10^{-3}
1	20	15,100	218
2	17.5	13,200	379
3	15	11,320	1,048
4	14	10,560	3,452
5	13	9,820	6,277
6	12	9,060	11,096
7	10	7,550	31,802*

* Removed before failure.

TABLE IX

S-N Data for 2014-T

400°F, Un-Notched

Specimen Number	Applied Load lb	S Stress psi	N No. of Cycles X 10^{-3}
1	40	30,200	181
2	35	26,400	739
3	30	22,650	2,575
4	27.5	20,750	3,520
5	"	"	2,546
6	"	"	3,053
7	"	"	6,465
8	"	"	2,430
9	25	18,850	7,106
10	"	"	4,714
11	23	17,350	8,805
12	22	16,600	19,503
13	21	15,850	34,688

TABLE X

S-N Data for 2014-T

400°F, 0.09 Radius Notch

Specimen Number	Applied Load lb	S Stress psi	N No. of Cycles X 10^{-3}
1	30	22,650	385
2	27.5	20,750	375
3	25	18,850	1,141
4	20	15,100	3,569
5	"	"	2,757
6	18.5	13,950	6,614
7	17	12,820	15,901
8	"	"	6,429
9	"	"	13,633
10	15	11,320	28,752
11	"	"	26,038
12	14.5	10,930	49,384

TABLE XI

S-N Data for 2014-T

400°F, 0.02 Radius Notch

Specimen Number	Applied Load lb	S Stress psi	N No. of Cycles X 10^{-3}
1	25	18,850	137
2	20	15,100	652
3	17.5	13,200	1,188
4	15	11,320	2,080
5	14	10,560	3,027
6	13	9,820	9,951
7	12	9,060	13,570
8	11	8,300	10,680
9	"	"	46,799

TABLE XII

S-N Data for 2014-T

400°F, 0.01 Radius Notch

Specimen Number	Applied Load lb	S Stress psi	N No. of Cycles X 10^{-3}
1	20	15,100	217
2	16.5	12,450	577
3	15	11,320	731
4	14	10,560	1,087
5	12	9,060	3,659
6	11	8,300	4,890
7	10	7,550	5,330
8	"	"	2,165
9	8.94	6,750	4,994
10	"	"	12,988
11	8.44	6,370	5,315
12	"	"	27,252
13	8.12	6,130	48,765*

*Removed before failure.

TABLE XIII

S-N Data for 7075-T

Room Temperature, Un-Notched

Specimen Number	Applied Load lb	S Stress psi	N No. of Cycles X 10^{-3}
1	60	45,300	161
2	55	41,500	188
3	50	37,750	386
4	45	34,000	904
5	42.5	32,100	44,557
6	"	"	22,023
7	"	"	5,013
8	40	30,200	1,628
9	"	"	20,800
10	"	"	2,402
11	"	"	8,323
12	"	"	946
13	37.5	28,300	1,020
14	"	"	1,264
15	"	"	33,568
16	"	"	124,386
17	35	26,400	1,776
18	"	"	35,070
19	"	"	78,937

TABLE XIV

S-N Data for 7075-T

Room Temperature, 0.09 Radius Notch

Specimen Number	Applied Load lb	S Stress psi	N No. of Cycles X 10^{-3}
1	45	33,950	62
2	"	"	30
3	40	30,200	276
4	35	26,400	340
5	34	25,650	512
6	32.5	24,500	4,935
7	32	24,150	1,585
8	"	"	8,119
9	31	23,400	7,741
10	30	22,650	11,047
11	25	18,850	38,532

TABLE XV

S-N Data for 7075-T

Room Temperature, 0.02 Radius Notch

Specimen Number	Applied Load lb	S Stress psi	N No. of Cycles X 10^{-3}
1	35	26,400	50
2	30	22,650	154
3	28	21,100	429
4	25	18,850	588
5	22.5	17,000	219
6	"	"	535
7	22	16,600	5,718
8	20	15,100	3,646
9	"	"	6,407
10	19	14,320	46,274
11	18	13,580	5,042
12	"	"	49,629
13	15	11,320	164,376*

* Removed before failure.

TABLE XVI

S-N Data for 7075-T

Room Temperature, 0.01 Radius Notch

Specimen Number	Applied Load lb	S Stress psi	N No. of Cycles X 10^{-3}
1	30	22,650	68
2	25	18,850	301
3	20	15,100	674
4	"	"	554
5	17.5	13,200	1,749
6	16.5	12,450	7,844
7	15	11,320	18,076
8	13.5	10,180	69,030*

* Removed before failure.

TABLE XVII

S-N Data for 7075-T

200 Degrees F, Un-Notched

Specimen Number	Applied Load lb	S Stress psi	N No. of Cycles X 10^{-3}
1	55	41,500	203
2	50	37,750	401
3	45	34,000	1,319
4	40	30,200	1,662
5	"	"	5,855
6	37.5	28,300	6,509
7	35	26,400	11,757
8	"	"	9,044
9	32.5	24,500	43,661

TABLE XVIII

S-N Data for 7075-T

200 Degrees F, 0.09 Radius Notch

Specimen Number	Applied Load lb	S Stress psi	N No. of Cycles X 10^{-3}
1	40	30,200	124
2	35	26,400	329
3	30	22,650	465
4	29	21,850	700
5	28	21,100	3,962
6	27.5	20,750	2,485
7	26.5	20,000	5,584
8	26	19,620	11,337
9	25	18,850	21,268
10	23.5	17,720	66,490*

* Removed before failure.

TABLE XIX

S-N Data for 7075-T

200 Degrees F, 0.02 Radius Notch

Specimen Number	Applied Load lb	S Stress psi	N No. of Cycles X 10^{-3}
1	30	22,650	104
2	25	18,850	328
3	20	15,100	1,313
4	19	14,320	1,656
5	"	"	2,733
6	"	"	10,612
7	18	13,580	20,406
8	17	12,820	17,702
9	15	11,320	61,475

TABLE XX

S-N Data for 7075-T

200 Degrees F, 0.01 Radius Notch

Specimen Number	Applied Load lb	S Stress psi	N No. of Cycles X 10^{-3}
1	25	18,850	192
2	20	15,100	298
3	17.5	13,200	474
4	16	12,080	3,504
5	15	11,320	3,738
6	14.5	10,930	5,102
7	14	10,560	20,831

TABLE XXI

S-N Data for 7075-T

400 Degrees F, Un-Notched

Specimen Number	Applied Load lb	S Stress psi	N No. of Cycles X 10^{-3}
1	45	33,950	209
2	40	30,200	542
3	37.5	28,300	5,439
4	"	"	12,721
5	"	"	4,667
6	35	26,400	744
7	"	"	3,708
8	"	"	4,388
9	30	22,650	3,046
10	"	"	18,791
11	27.5	20,750	64,116
12	"	"	24,209
13	25	18,850	8,873
14	22.5	17,000	64,434
15	20	15,100	68,450*

* Removed before failure.

TABLE XXII

S-N Data for 7075-T

400 Degrees F, 0.09 Radius Notch

Specimen Number	Applied Load lb	S Stress psi	N No. of Cycles X 10^{-3}
1	35	26,400	210
2	31	23,400	494
3	"	"	180
4	30	22,650	535
5	27.5	20,750	662
6	"	"	459
7	25	18,850	3,095
8	23.5	17,720	4,185
9	22.5	17,000	1,467
10	"	"	3,773
11	20	15,100	4,137
12	"	"	10,356
13	17	12,820	9,093
14	16	12,080	24,017
15	15	11,320	33,310*

* Removed before failure.

TABLE XXIII

S-N Data for 7075-T

400 Degrees F, 0.02 Radius Notch

Specimen Number	Applied Load lb	S Stress psi	N No. of Cycles X 10^{-3}
1	25	18,850	86
2	20	15,100	519
3	"	"	311
4	"	"	611
5	17.5	13,200	932
6	17	12,820	1,569
7	"	"	1,746
8	15	11,320	5,705
9	14.5	10,930	4,440
10	13.5	10,180	8,119
11	12.5	9,440	13,307
12	11.5	8,775	9,737
13	"	"	22,291
14	11	8,300	16,172
15	10.5	7,930	19,703

TABLE XXIV

S-N Data for 7075-T

400 Degrees F, 0.01 Radius Notch

Specimen Number	Applied Load lb	S Stress psi	N No. of Cycles X 10^{-3}
1	25	18,850	83
2	20	15,100	360
3	17.5	13,200	270
4	15	11,320	415
5	14	10,560	1,231
6	13	9,820	1,255
7	12	9,060	5,308
8	"	"	1,024
9	"	"	5,126
10	"	"	7,653
11	11.5	8,775	8,375
12	11	8,300	10,948
13	10.5	7,920	11,887
14	10	7,550	15,435
15	"	"	10,889
16	"	"	22,068
17	9.43	7,120	67,629

TABLE XXV

Notch Sensitivity - q,

Theoretical Stress Concentration factor - K_t,

and Experimental Stress Concentration factor - K_f,

for 2014-T

Temperature (°F)	Room Temperature	200°	400°
<u>0.09 Notch</u>			
K_t	1.395	1.395	1.395
K_f	1.307	1.41	1.358
q	.788	1.036	.907
<u>0.02 Notch</u>			
K_t	2.27	2.27	2.27
K_f	1.702	1.883	1.855
q	.552	.695	.673
<u>0.01 Notch</u>			
K_t	3.0	3.0	3.0
K_f	2.195	2.35	2.351
q	.598	.675	.676

TABLE XXVI

Notch Sensitivity - q,

Theoretical Stress Concentration factor - K_t,

and Experimental Stress Concentration factor - K_f,

for 7075-T

Temperature (°F)	Room Temperature	200°	400°
<u>0.09 Notch</u>			
K_t	1.395	1.395	1.395
K_f	1.336	1.43	1.527
q	.851	1.088	1.332
<u>0.02 Notch</u>			
K_t	2.27	2.27	2.27
K_f	1.993	2.051	2.172
q	.781	.828	.924
<u>0.01 Notch</u>			
K_t	3.0	3.0	3.0
K_f	2.354	2.477	2.631
q	.677	.739	.815

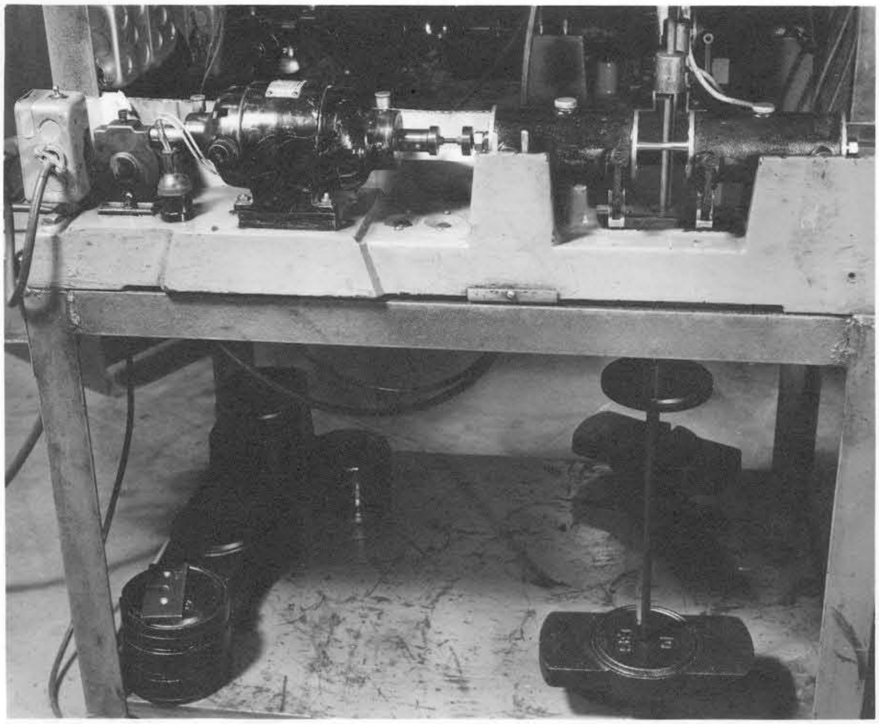

Fig. 1

R. R. Moore Machine

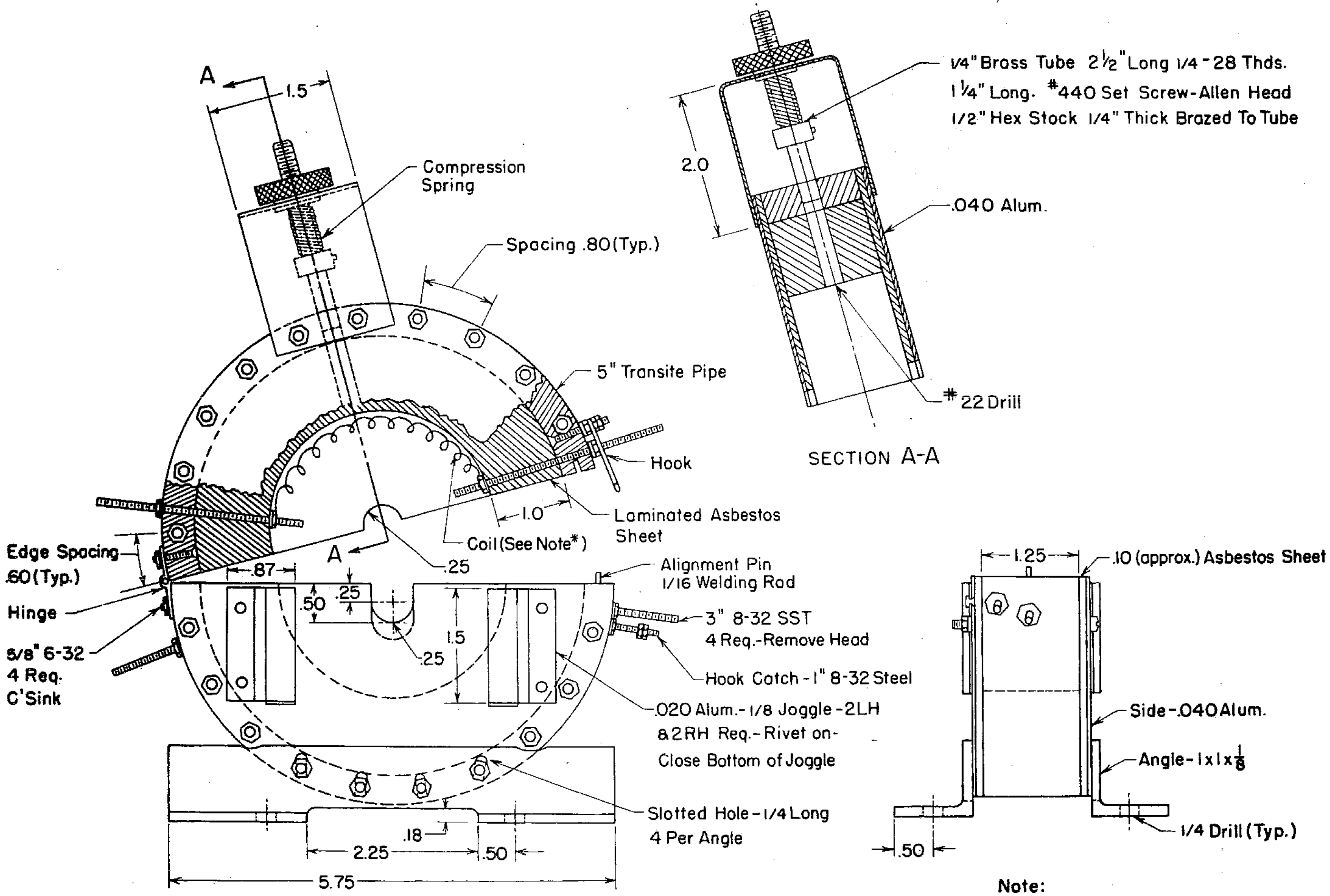

Note:

1. *Coil - 48" No.23 Tophet-C wound into flat coil - 1.10 wide x .20 (approx.) deep.
2. All dimensions inches

FURNACE FOR R.R. MOORE
FATIGUE TESTING MACHINE
FIG. 2

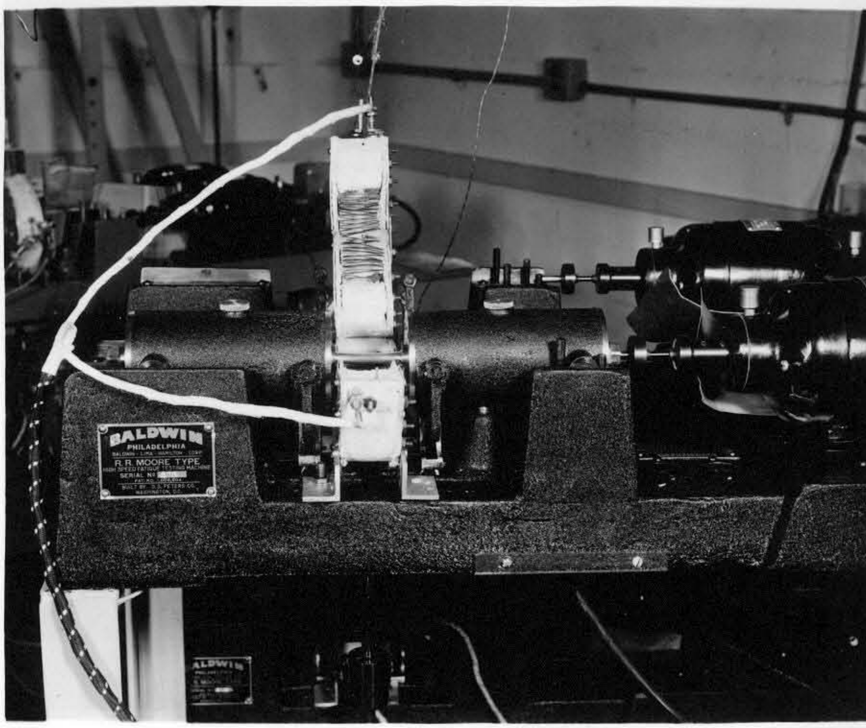

Fig. 3

Furnace for Use with

R. R. Moore Machine - Open

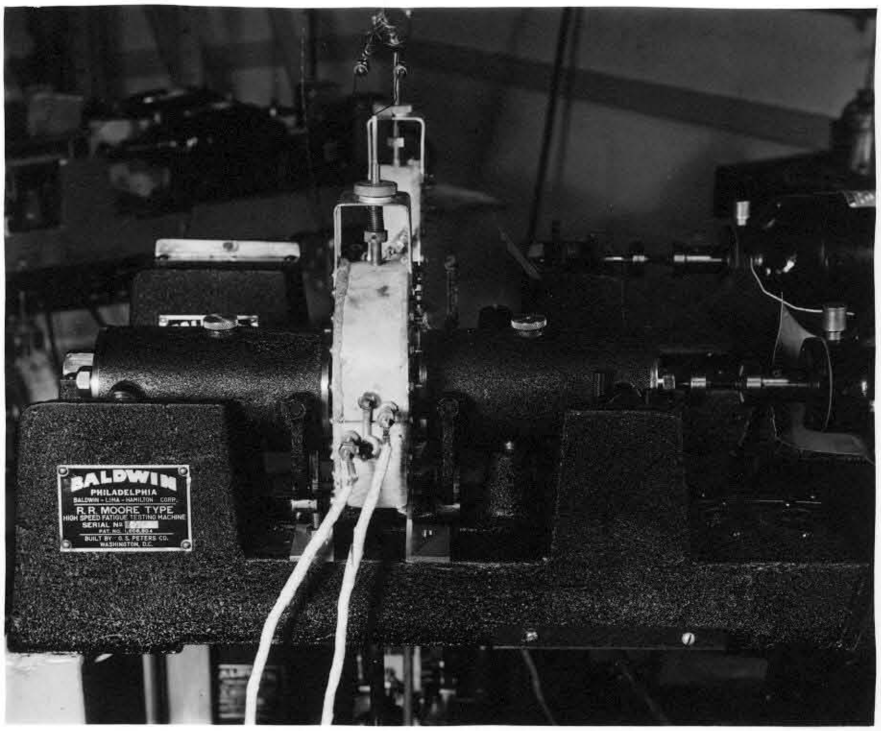

Fig. 4

Furnace for Use with

R. R. Moore Machine - Closed

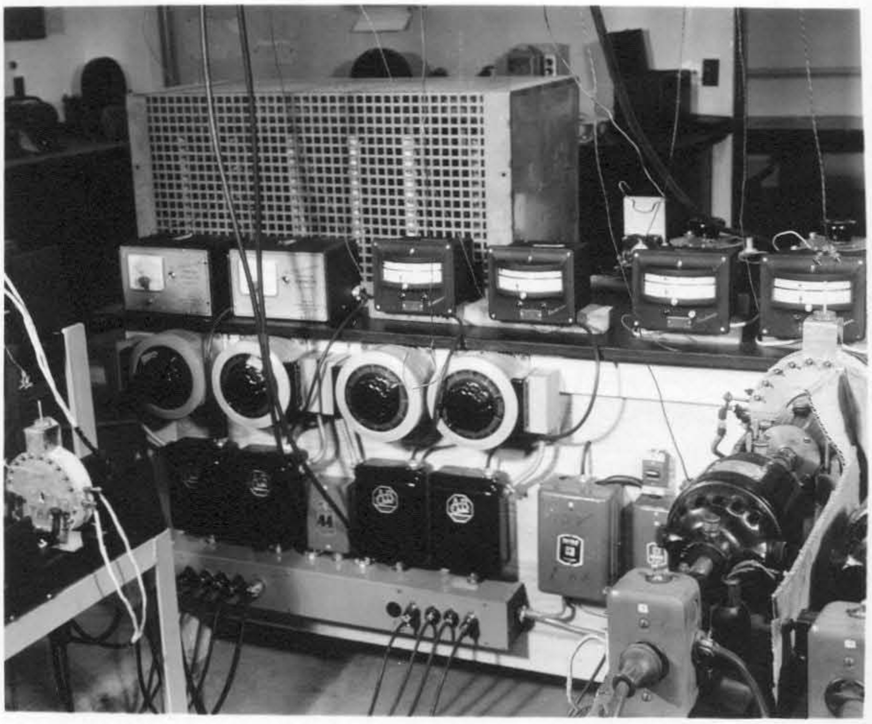

Fig. 5

General View of Control Table

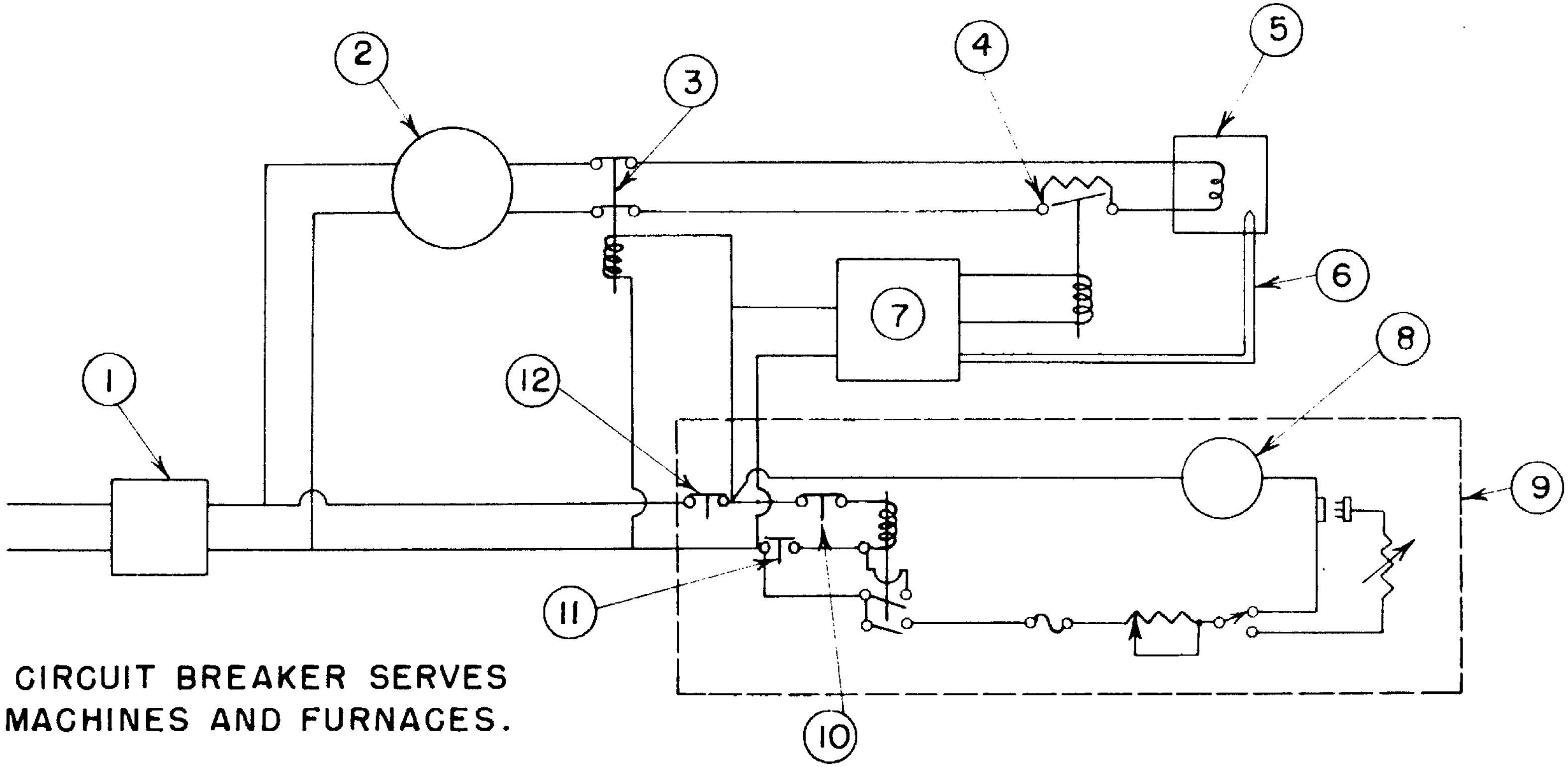

NOTE:
EACH CIRCUIT BREAKER SERVES TWO MACHINES AND FURNACES.

(1) CIRCUIT BREAKER
(2) POWERSTAT
(3) FURNACE CUT-OFF RELAY
(4) FURNACE CUT-OFF RELAY AND BALLAST RESISTOR
(5) FURNACE
(6) THERMOCOUPLE
(7) PYROMETER
(8) MOTOR
(9) R.R.MOORE MACHINE
(10) STOP SWITCH
(11) START SWITCH
(12) SPECIMEN FAILURE CUT-OFF SWITCH

FIG. 6

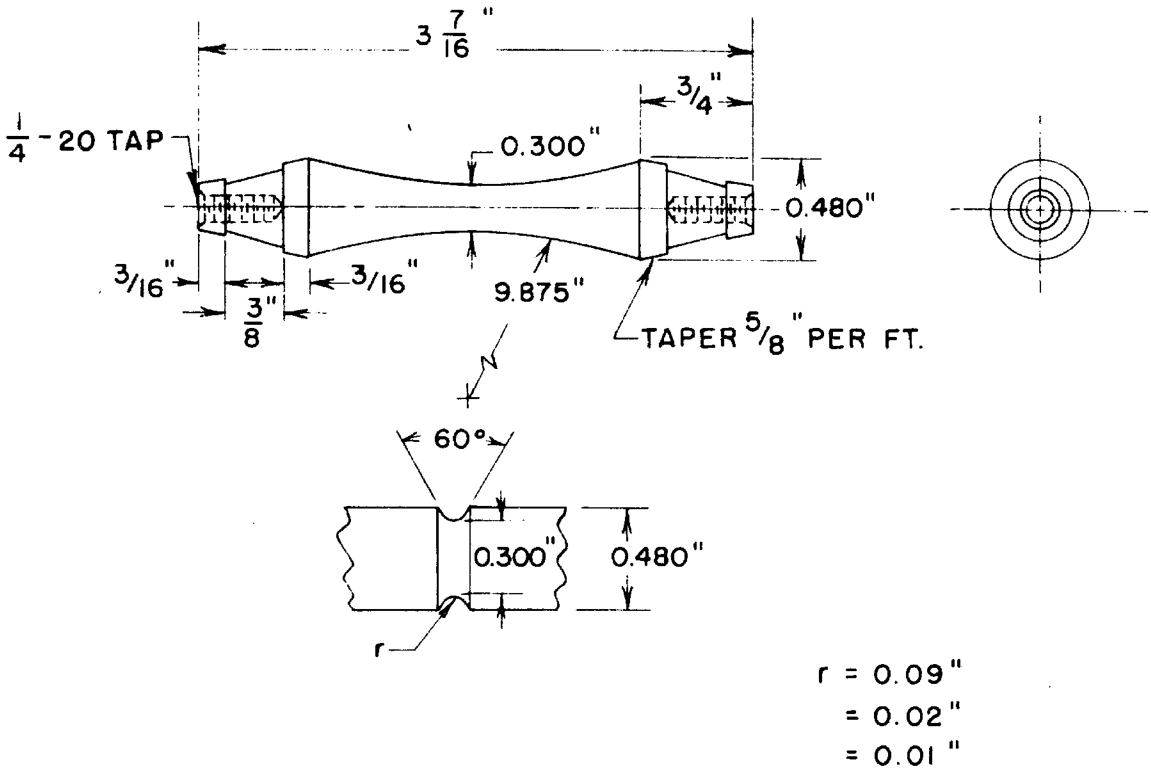

FIG. 7 - ASTM STANDARD SPECIMENS FOR R.R. MOORE TESTING MACHINE

SYMBOLOGY FOR FIGURES 8 THROUGH 13

○ - Specimens not notched.

△ - 0.09 inch radius notch.

□ - 0.02 inch radius notch.

▽ - 0.01 inch radius notch.

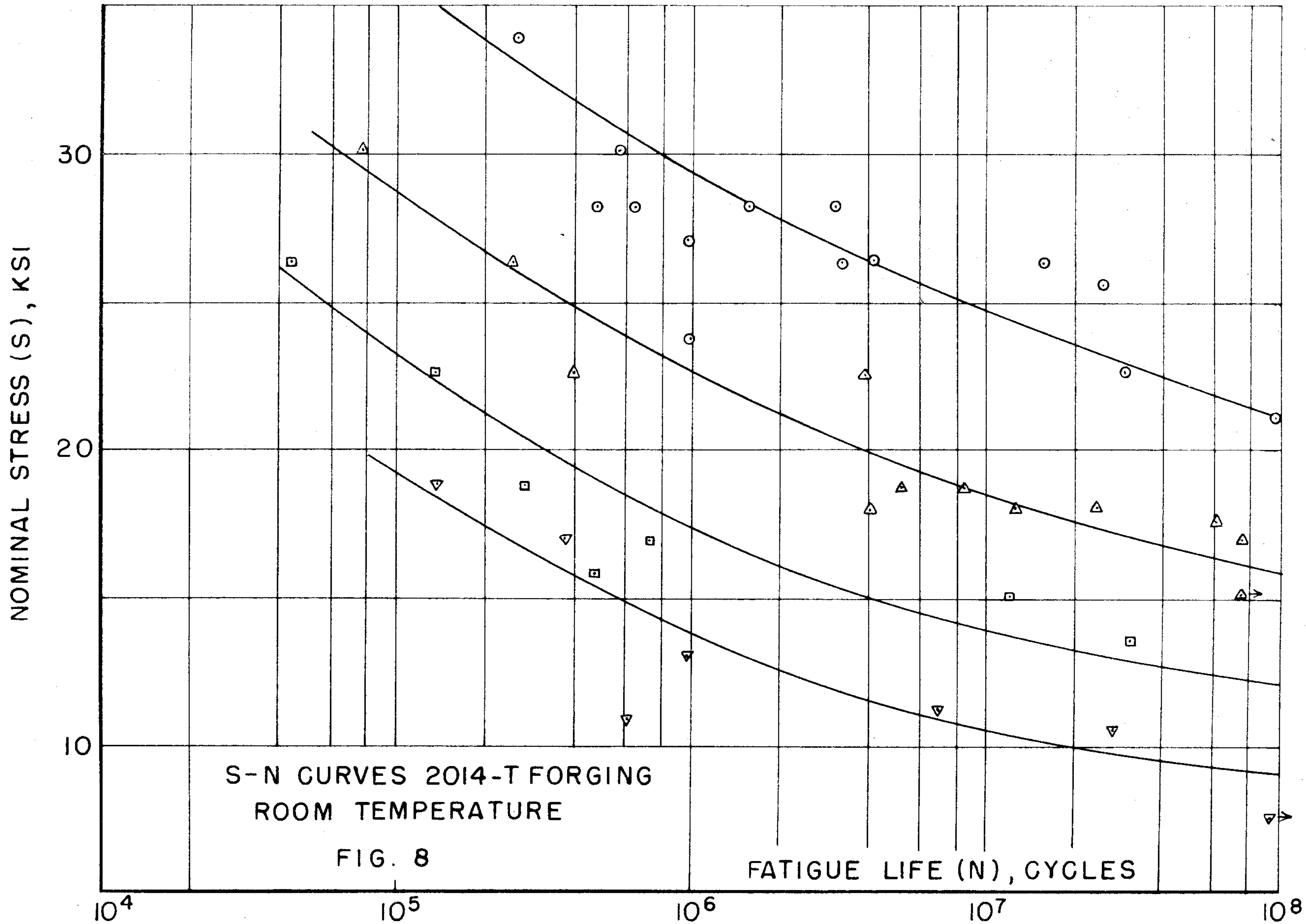

S-N CURVES 2014-T FORGING
ROOM TEMPERATURE

FIG. 8

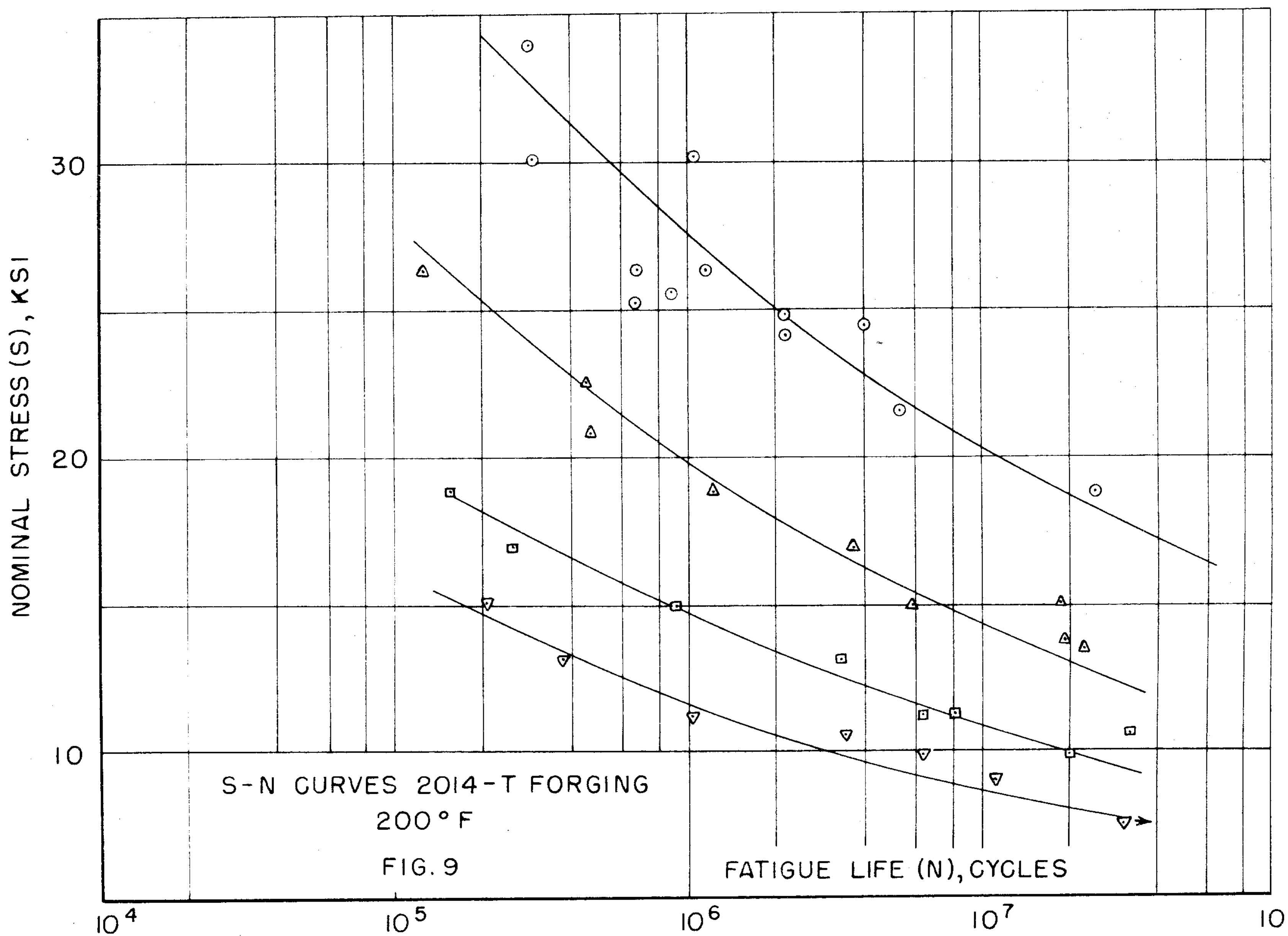

S-N CURVES 2014-T FORGING
200° F

FIG. 9

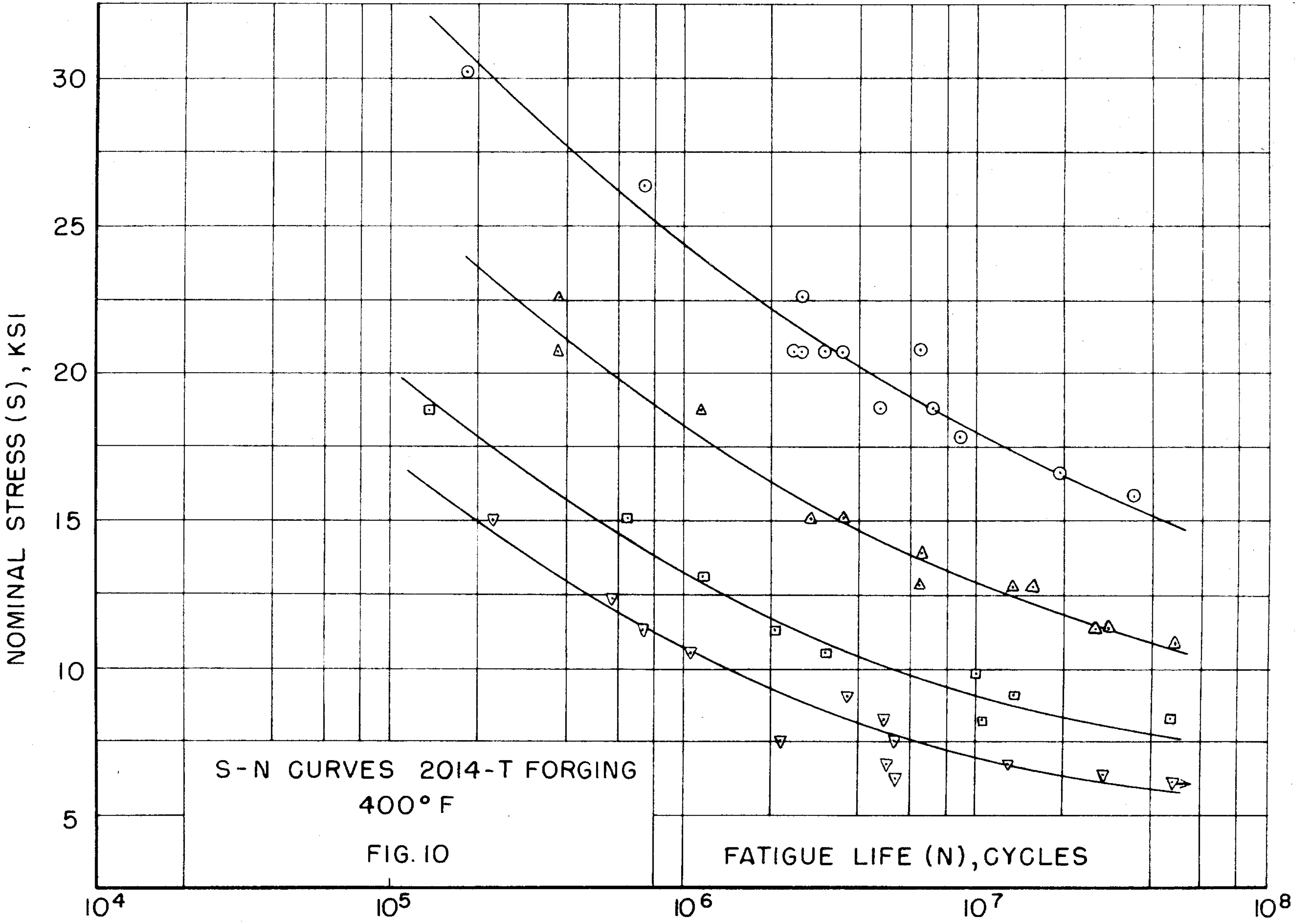

S-N CURVES 2014-T FORGING
400° F

FIG. 10

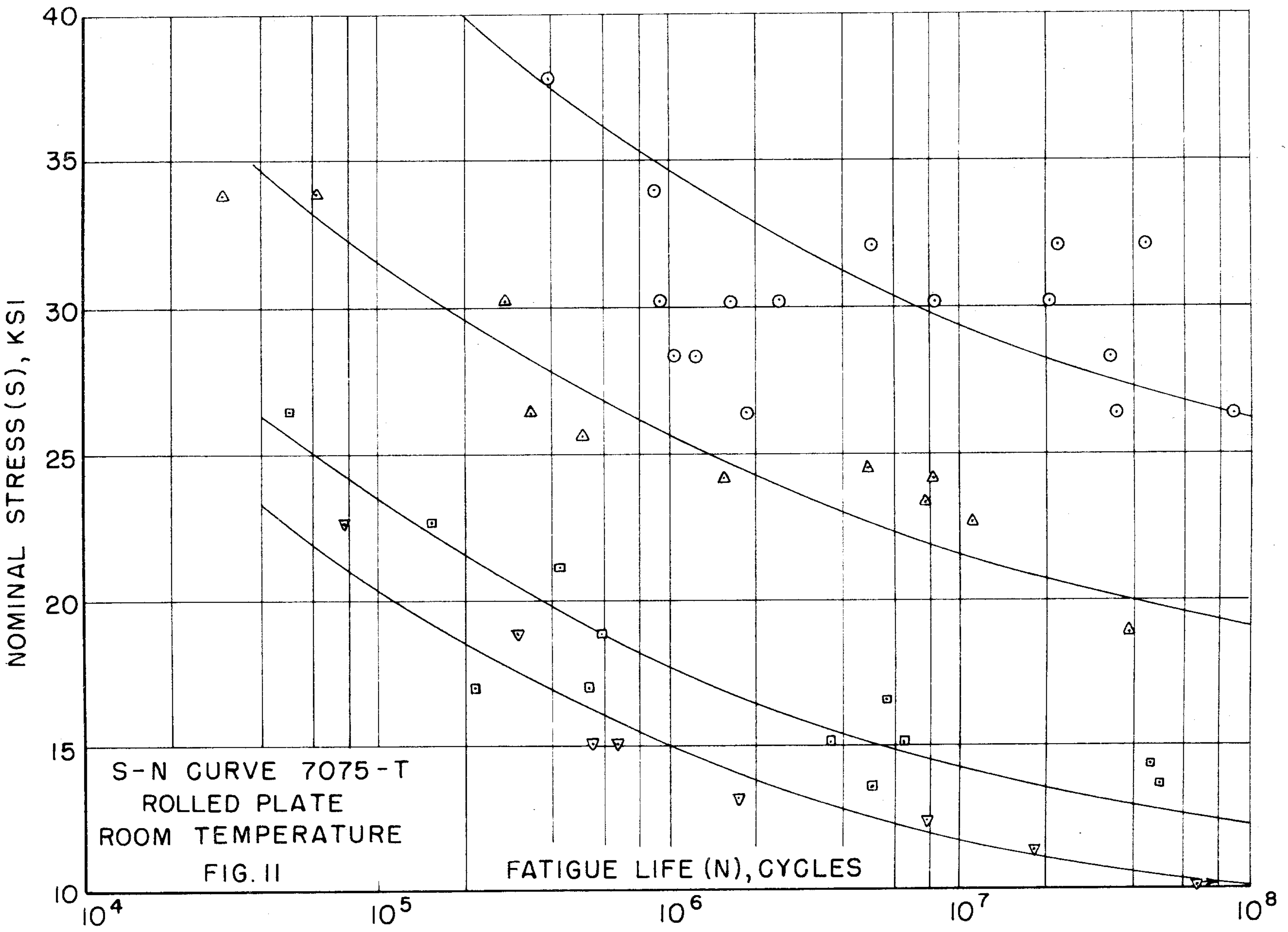

S-N CURVE 7075-T
ROLLED PLATE
ROOM TEMPERATURE
FIG. 11

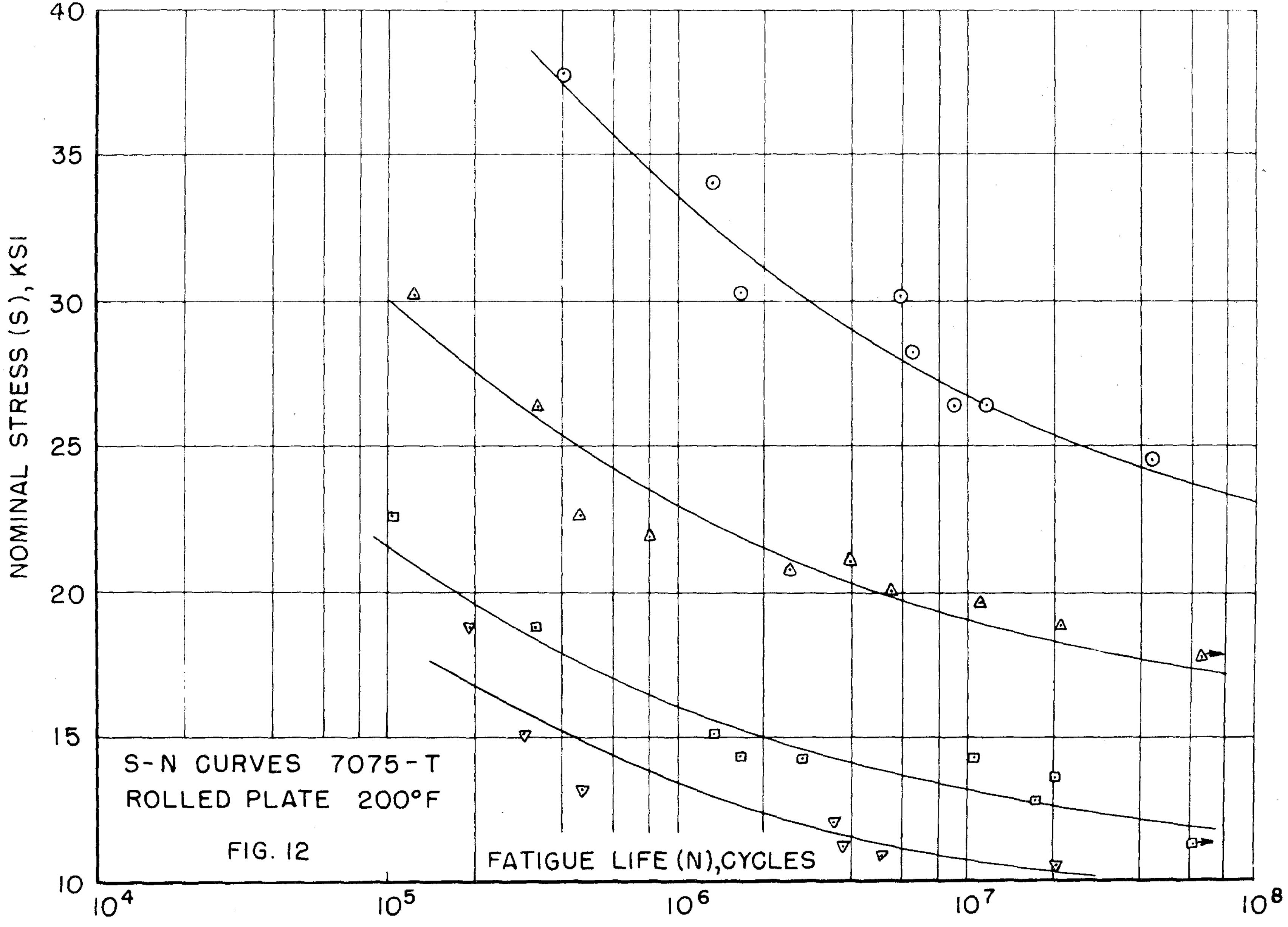
S-N CURVES 7075-T
ROLLED PLATE 200°F
NOMINAL STRESS (S), KSI
FATIGUE LIFE (N), CYCLES
40
35
30
25
20
15
10
10^4
10^5
10^6
10^7
10^8

FIG. 12

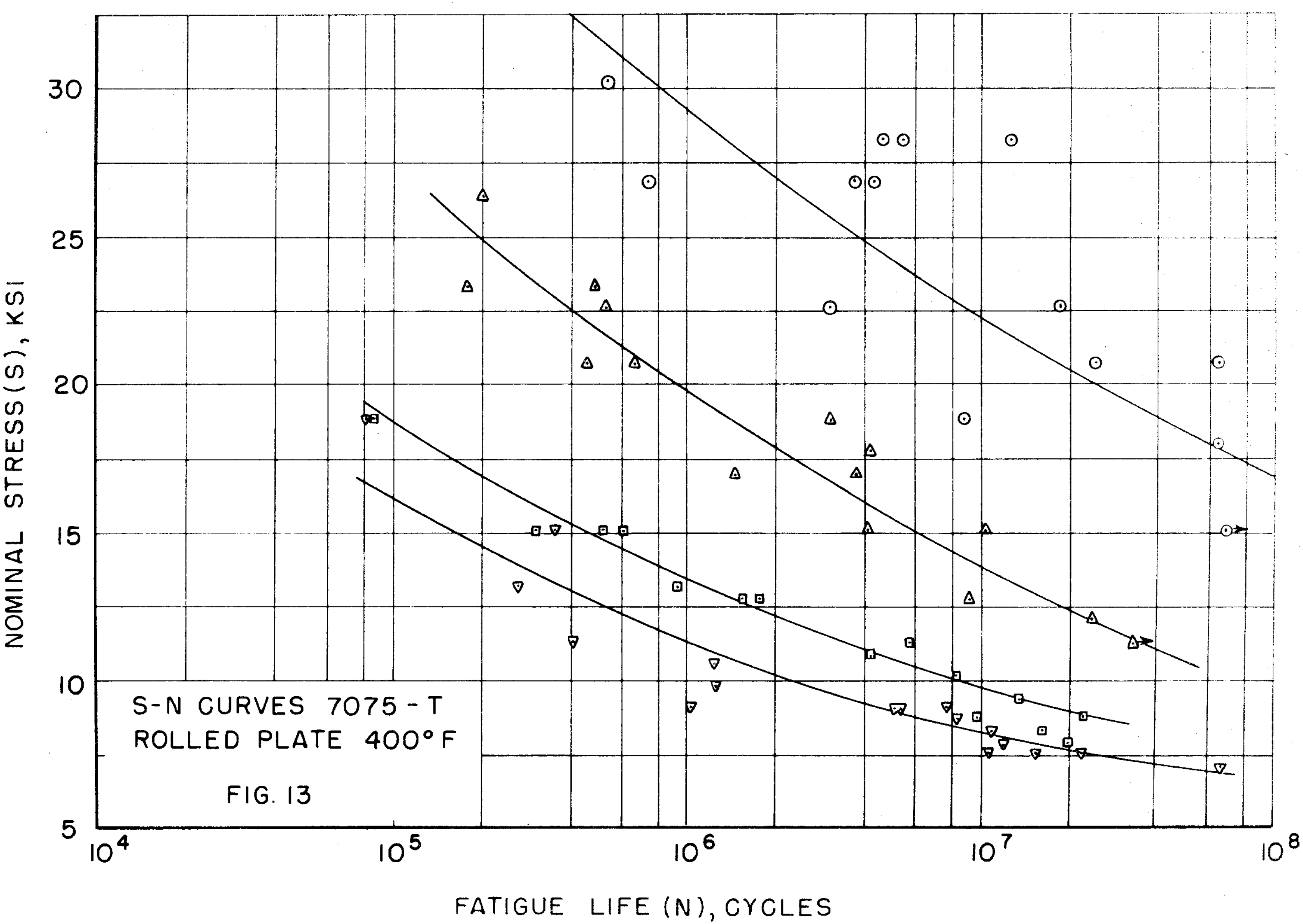

S-N CURVES 7075-T
ROLLED PLATE 400°F

FIG. 13

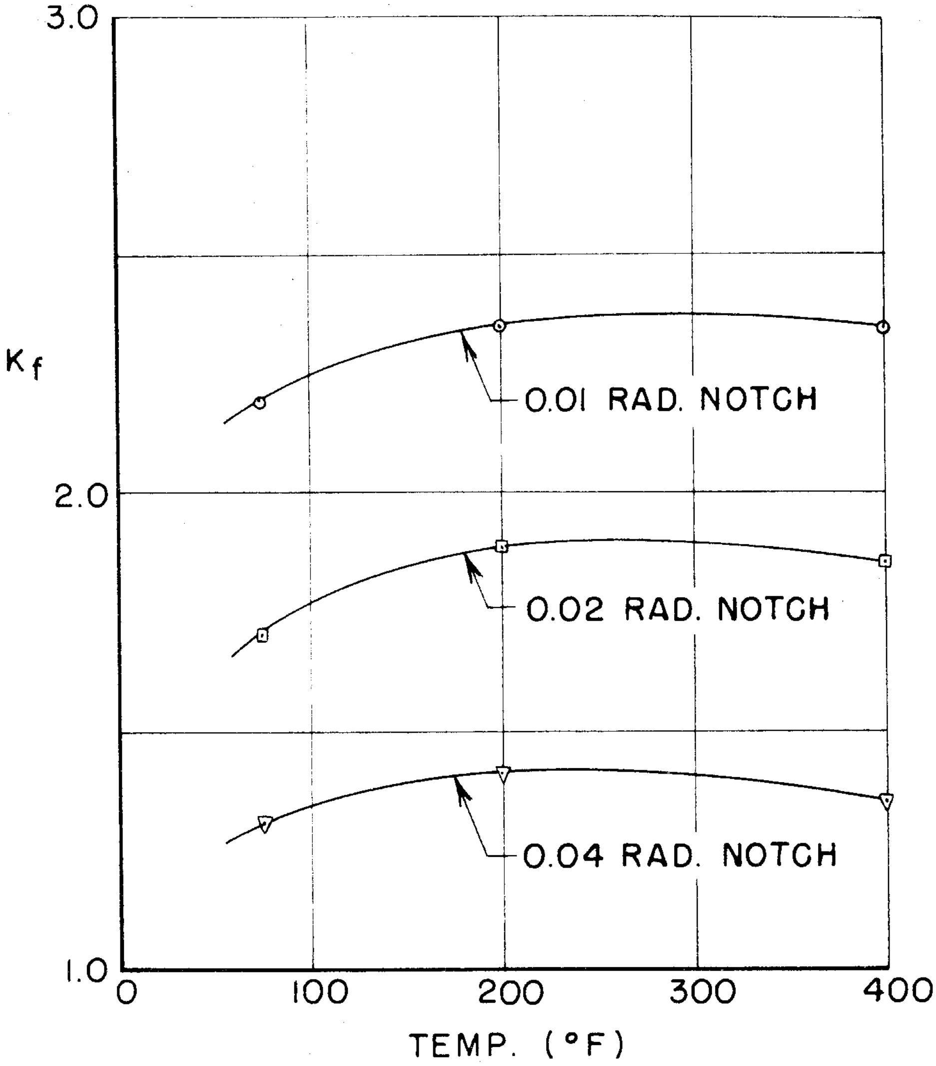

FIG. 14 – VARIATION OF EXPERIMENTAL FATIGUE STRESS CONCENTRATION FACTOR vs. TEMPERATURE FOR 2014 FORGING

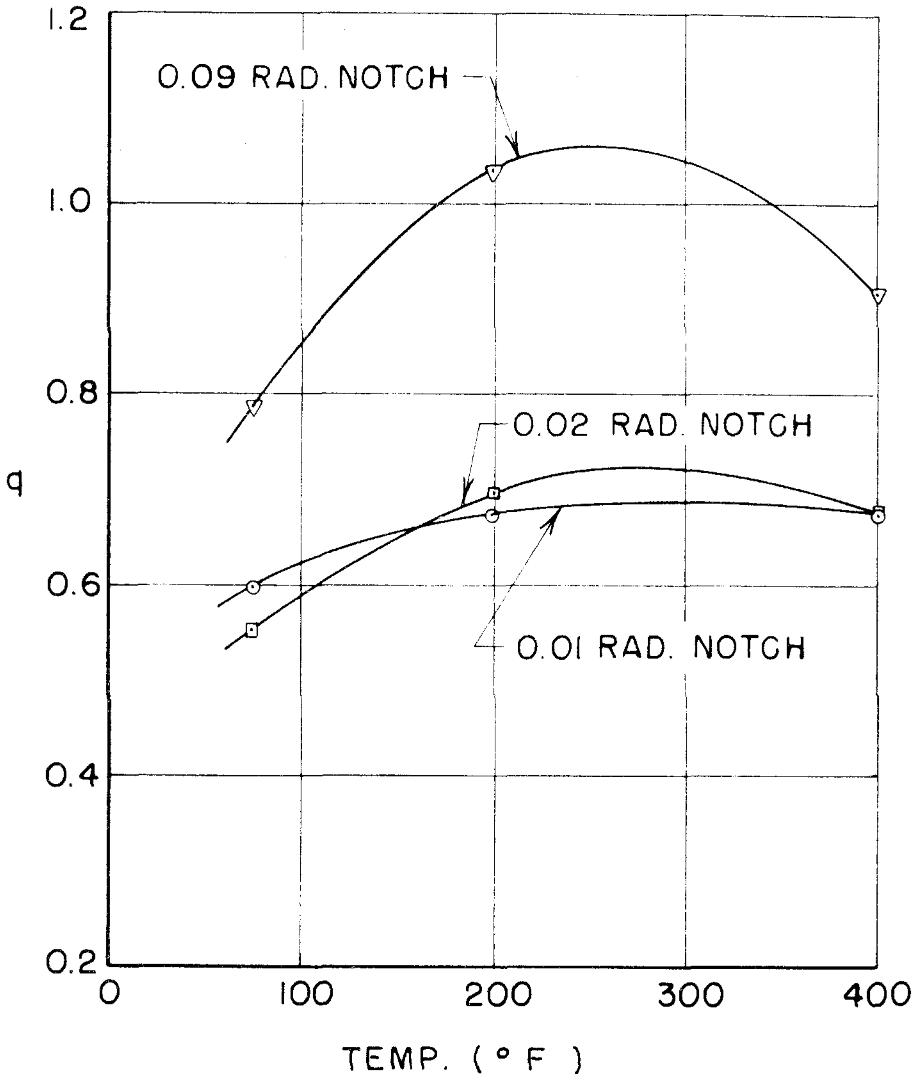

FIG. 15 – NOTCH SENSITIVITY FACTOR vs. TEMPERATURE FOR 2014-T FORGING

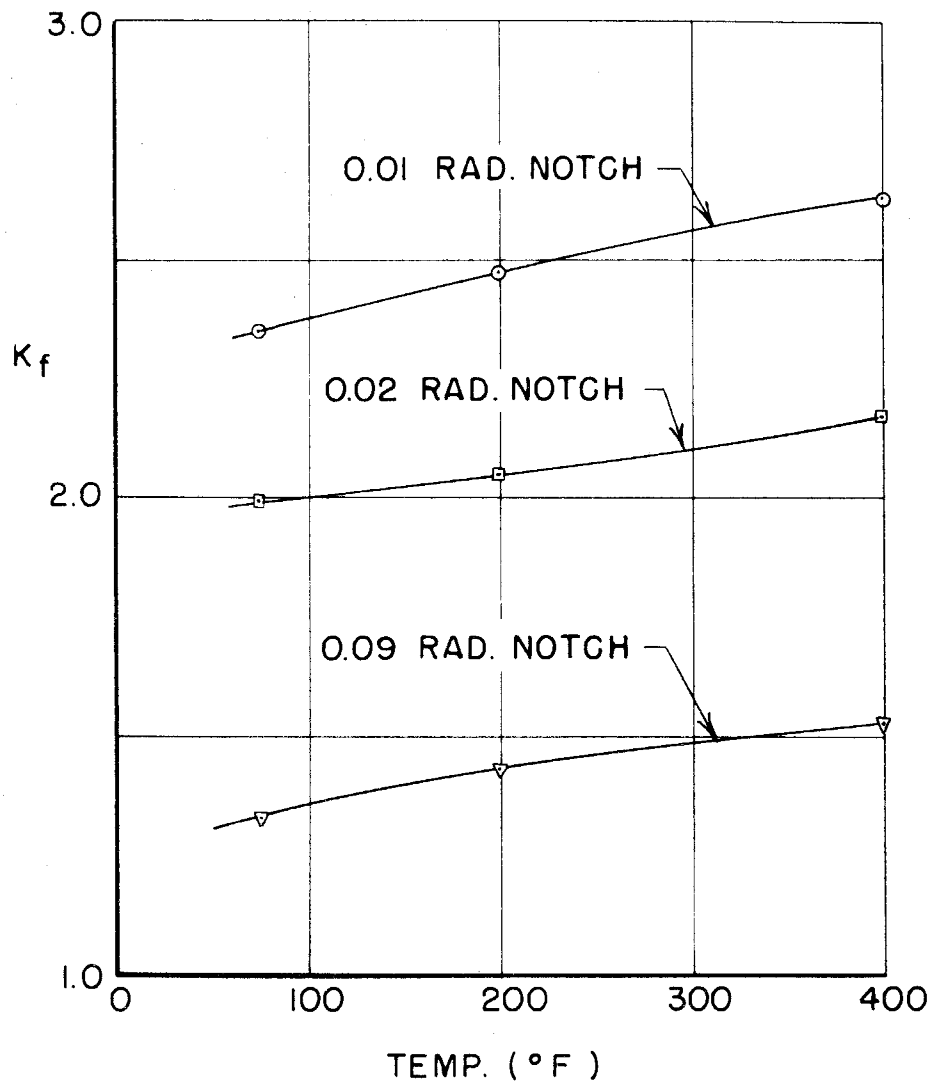

FIG. 16 - VARIATION OF EXPERIMENTAL FATIGUE STRESS CONCENTRATION FACTOR vs. TEMPERATURE FOR 7075-T ROLLED PLATE

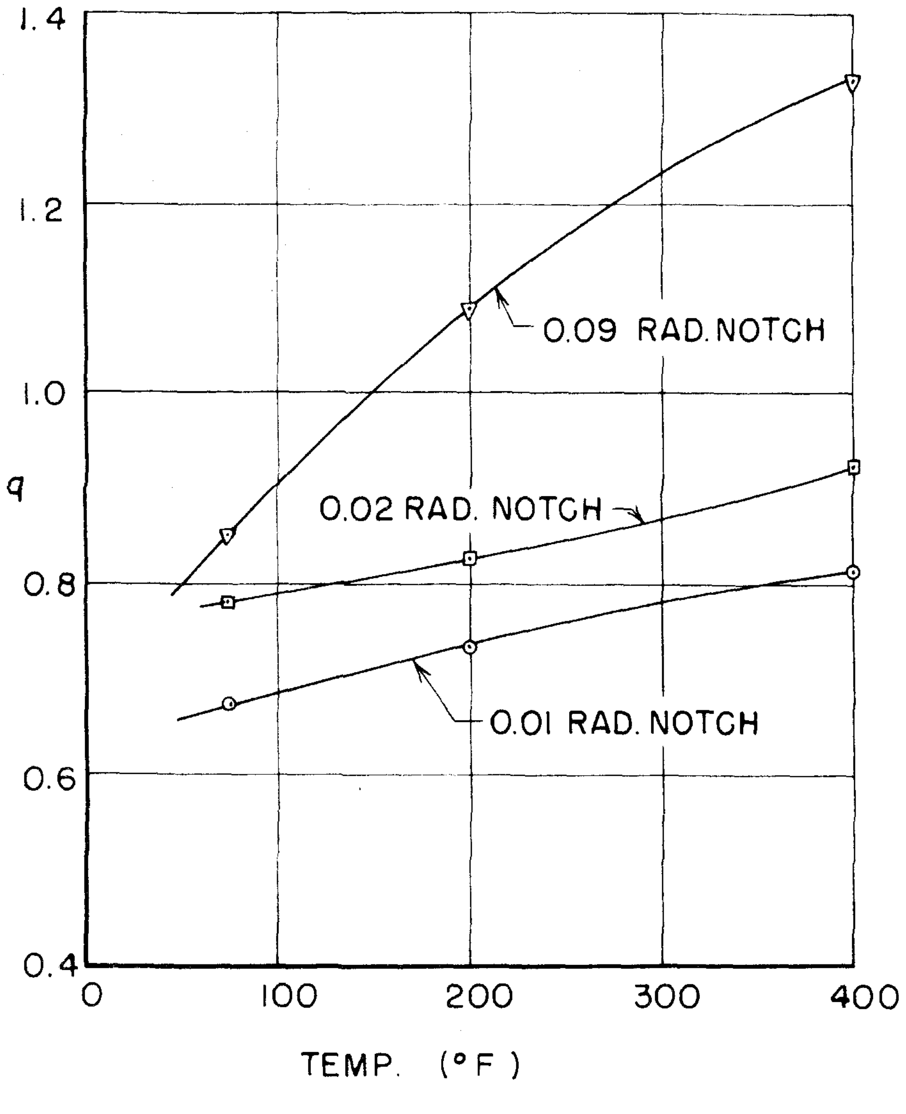

FIG. 17 – NOTCH SENSITIVITY FACTOR vs. TEMPERATURE FOR 7075 - T ROLLED PLATE